JACC: BASIC TO TRANSLATIONAL SCIENCE VOL. 9, NO. 7, 2024

LEADING EDGE TRANSLATIONAL RESEARCH

Human Aortic Stenotic Valve-Derived Extracellular Vesicles Induce Endothelial Dysfunction and Thrombogenicity Through AT1R/NADPH Oxidases/SGLT2 Pro-Oxidant Pathway

Sandy Hmadeh, PhD,[a] Antonin Trimaille, MD, MSc,[a,b] Kensuke Matsushita, MD, PhD,[a,b] Benjamin Marchandot, MD,[b] Adrien Carmona, MD,[b] Fatiha Zobairi, BSc,[a] Chisato Sato, MD, PhD,[a,b] Michel Kindo, MD, PhD,[b] Tam Minh Hoang, MD,[b] Florence Toti, PhD,[a] Kazem Zibara, PhD,[c] Eva Hamade, PhD,[c] Valérie Schini-Kerth, PhD,[a] Gilles Kauffenstein, PhD,[a] Olivier Morel, MD, PhD[a,b,d]

VISUAL ABSTRACT

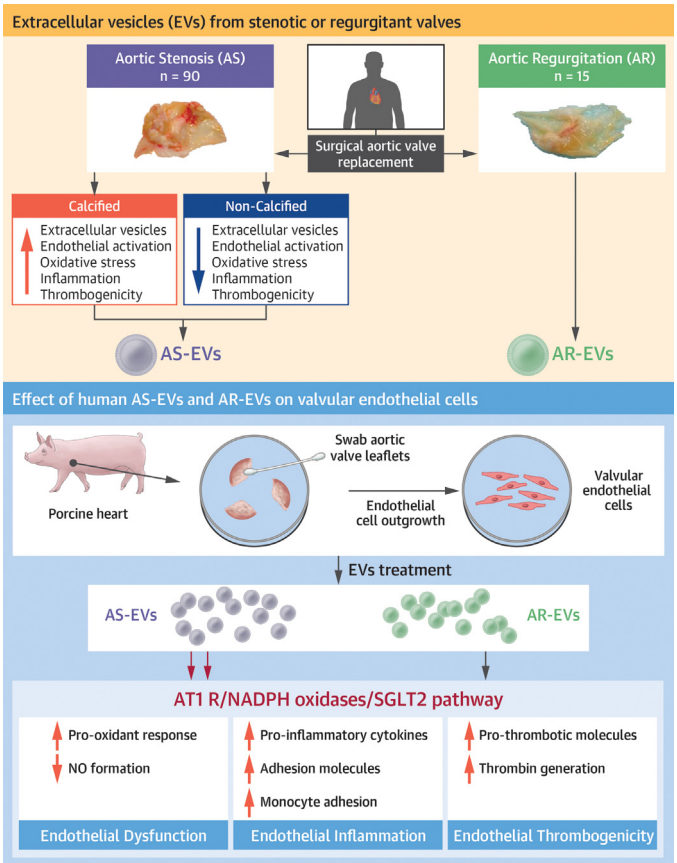

Hmadeh S, et al. JACC Basic Transl Sci. 2024;9(7):845-864.

HIGHLIGHTS

- **Subclinical leaflet thrombosis was recently linked to higher rates of stroke and transient ischemic attack after TAVR. EVs have emerged as a surrogate marker of endothelial dysfunction and cardiovascular risk.**
- **This study demonstrates the role of EVs trapped within the native aortic valve in valvular dysfunction and thrombogenicity, and points at the contribution of the local angiotensin system/NADPH oxidases/SGLT2 pro-oxidant pathway.**
- **Additional studies will be required to clarify the impact of SGLT2 in the limitation of EV-mediated injuries in patients with AS or following TAVR.**

ISSN 2452-302X https://doi.org/10.1016/j.jacbts.2024.02.012

JACC: BASIC TO TRANSLATIONAL SCIENCE VOL. 9, NO. 7, 2024
JULY 2024:845–864

ABBREVIATIONS AND ACRONYMS

ACE = angiotensin-converting enzyme

Ang II = angiotensin II

AR = aortic regurgitation

AS = aortic stenosis

eNOS = endothelial nitric oxide synthase

EV = extracellular vesicle

HBSS = Hanks' balanced salt solution

NO = nitric oxide

RBC = red blood cell

SAVR = surgical aortic valve replacement

SGLT2 = sodium-glucose co-transporter 2

TAVR = transcatheter aortic valve replacement

TF = tissue factor

VEC = valvular endothelial cell

VIC = valvular interstitial cell

SUMMARY

Pathological tissues release a variety of factors, including extracellular vesicles (EVs) shed by activated or apoptotic cells. EVs trapped within the native pathological valves may act as key mediators of valve thrombosis. Human aortic stenosis EVs promote activation of valvular endothelial cells, leading to endothelial dysfunction, and proadhesive and procoagulant responses. (JACC Basic Transl Sci 2024;9:845–864)

Aortic stenosis (AS) is the most common valvular heart disease in industrialized countries, where its increased prevalence is driven by population aging. Although AS was previously viewed as a passive degenerative process, current evidence suggests that its pathogenesis is intricated and highly dynamic.[1,2] This interplay ultimately leads to a cascade of events, including oxidative stress, endothelial dysfunction, lipid deposition, inflammation, osteoblastic differentiation, and finally, valve calcification.[1,3] Understanding the pathophysiology of AS and the underlying biological processes of the stenotic valve are essential for identifying targeted treatments to slow disease progression or to prevent leaflet thrombosis and structural valve deterioration following transcatheter aortic valve replacement (TAVR).[4,5] Recent data have highlighted that native aortic valves exhibit evidence of ongoing disease activity (elevated ^{18}F-NaF uptake), potentially linked to disease progression,[6] and could therefore constitute an important reservoir of bioactive material.

In the setting of cardiovascular disease, pathological tissues release a variety of factors, including extracellular vesicles (EVs) shed by activated or apoptotic cells. EVs can serve as powerful biological shuttles that orchestrate cellular cross-talk and critical biological responses in neighboring tissues.[7]

In the present study, we hypothesized that EVs trapped within the native pathological valves may act as key mediators of valve dysfunction and thrombosis. To investigate this, we studied ex vivo the generation of EVs from AS (AS-EVs) and aortic regurgitation (AR-EVs) human valves, and determined the importance of tissue calcification and activation including oxidative stress, inflammation, and endothelial cell activation. Using an in vitro approach, we evaluated the potential of these EVs to promote activation of porcine valvular endothelial cells (VECs) leading to endothelial dysfunction, proadhesive and procoagulant responses, and characterized the role of the AT1R/NADPH oxidases/sodium-glucose co-transporter 2 (SGLT2) pro-oxidant pathway.

METHODS

The methods are extensively described in the Supplemental Appendix. Briefly, this prospective study enrolled 90 patients with AS and 15 patients with AR referred for surgical aortic valve replacement (SAVR) at the University Hospital of Strasbourg, France, between May 2019 and October 2021. The institutional review board approved all studies (IRB number: FC/2016-4), and all participants gave informed consent. Aortic valves from these patients were collected after surgery. Not all valves were used for the different experiments. Of the 105 valves collected, 14 valves were used for histological and immunofluorescent analysis, 13 valves for calcified vs noncalcified experimentations, and 78 valves were used for EVs quantification (65 valves from AS patients and 13 valves from AR patients) (Supplemental Figure 1). The lack of availability of all valves for each experiment is related to the characteristics of each protocol. Phenotypic characterization of the valves was made using Western blot analysis and immunofluorescence staining, and EVs were isolated and

From the [a]UR 3074 Translational Cardiovascular Medicine, CRBS, Strasbourg, France; [b]Department of Cardiovascular Medicine, Nouvel Hôpital Civil, Strasbourg University Hospital, Strasbourg, France; [c]Faculty of Sciences, Laboratory of Genomics and Health, Lebanese University, Hadath, Lebanon; and the [d]Hanoï Medical University, Hanoi, Vietnam.

The authors attest they are in compliance with human studies committees and animal welfare regulations of the authors' institutions and Food and Drug Administration guidelines, including patient consent where appropriate. For more information, visit the Author Center.

Manuscript received May 10, 2023; revised manuscript received February 22, 2024, accepted February 22, 2024.

TABLE 1 Main Clinical and Echocardiographic Features of Patients

	Whole Cohort (N = 105)	Aortic Stenosis (n = 90)	Aortic Regurgitation (n = 15)	*P* Value
Age, y	69.1 (61.9-74.2)	69.2 (63.1-74.1)	68.2 (50.7-73.2)	0.14
Male	70 (66.7)	61 (66.7)	9 (60.0)	0.55
BMI, 30 kg/m^2	28.4 (24.5-32.3)	28.4 (24.7-32.2)	26.1 (23.1-31.1)	0.32
Hypertension	68 (64.8)	59 (65.6)	9 (60.0)	0.68
Diabetes	17 (16.2)	15 (16.7)	2 (13.3)	>0.99
Dyslipidemia	57 (54.3)	54 (60.0)	3 (20.0)	<0.01
Smoking	5 (4.8)	4 (4.4)	1 (6.7)	0.54
CAD	23 (21.9)	23 (25.6)	0 (0.0)	0.04
Atrial fibrillation	17 (16.2)	15 (16.7)	2 (13.3)	>0.99
Stroke	3 (2.9)	2 (2.2)	1 (6.7)	0.59
CKD[a]	9 (8.6)	5 (5.6)	4 (26.7)	0.02
COPD	5 (4.8)	4 (4.4)	1 (6.7)	0.54
SAPT	46 (43.8)	41 (45.6)	5 (33.3)	0.38
OAC	16 (15.2)	12 (13.3)	4 (26.7)	0.24
ACEI	33 (31.4)	29 (32.2)	4 (26.7)	0.78
ARBs	22 (21.0)	19 (21.1)	3 (20.0)	>0.99
Beta-blocker	41 (39.0)	35 (38.9)	6 (40.0)	0.93
Statin	51 (48.6)	49 (54.4)	2 (13.3)	<0.01
Diuretic agents	12 (11.4)	9 (10.0)	3 (20.0)	0.37
Bicuspid valve	22 (21.0)	17 (18.8)	5 (33.3)	0.30
LVEF, %	61 (56-67)	61 (57-67)	61 (53-63)	0.33
Stroke volume, mL/m^2	45 (38-55)	44 (38-53)	65 (42-87)	0.016
LV hypertrophy	54 (51.4)	42 (46.7)	12 (80.0)	0.056
Mean transaortic gradient, mm Hg	46 (41-53)	47 (43-54)	12 (6-21)	<0.001
Vmax, cm/s	429 (396-466)	434 (407-470)	260 (213-300)	<0.001
Aortic surface, cm^2	0.9 (0.7-1.0)	0.9 (0.7-1.0)	2.2 (1.3-3.2)	0.004
Indexed aortic surface, cm^2/m^2	0.5 (0.4-0.5)	0.4 (0.3-0.5)	1.2 (0.8-1.5)	0.002
Permeability index, IU	0.23 (0.20-0.28)	0.2 (0.2-0.3)	0.6 (0.3-0.7)	0.001

Values are median (Q1-Q3) or n (%). Percentages are based on patients for whom data were available. The comparison was made between aortic stenosis and aortic regurgitation patients using the chi-squared or Fisher exact test for categorical variables, and using the Student's *t*-test or the Wilcoxon rank sum test according to the distribution of the continuous variables. [a]Chronic kidney disease (CKD) is defined as an estimated glomerular filtration rate ≤60 mL/min/1.73 m^2.

ACEI = angiotensin-converting enzyme inhibitor; ARBs = angiotensin receptor blockers; BMI = body mass index; CAD = coronary artery disease; COPD = chronic obstructive pulmonary disease; LV = left ventricle; LVEF = left ventricular ejection fraction; OAC = oral anticoagulant; SAPT = single antiplatelet therapy.

quantified by prothrombinase assay. In addition, primary cultures of porcine VECs were performed and treated with either AS-EVs or AR-EVs. Protein expression level was assessed by Western blot analysis (Supplemental Table 2) and immunofluorescence staining, mRNA levels by real-time quantitative polymerase chain reaction, oxidative stress using dihydroethidium, and the formation of nitric oxide (NO) using DAF-FM diacetate.

EVs ISOLATION FROM AORTIC VALVES, PLATELETS, AND ERYTHROCYTES. EVs from human pathological aortic valves were collected from fresh tissues by sequential centrifugation. Briefly, tissues were washed with Hanks' balanced salt solution (HBSS), excess fluid removed by adsorbent tissue, and then quickly weighed. Tissues were then sectioned into small squares of 1- to 2-mm sides using a razor blade and incubated in HBSS (300 mg of tissue/1 mL HBSS) using a rotating wheel (20 rpm) for 90 minutes at room temperature. Subsequently, the tissue was centrifuged at 800*g* for 15 minutes, and the pelleted tissue was frozen at −80°C for subsequent protein extraction and calcium content determination. The supernatant containing EVs was centrifuged twice at 13,000*g* for 5 minutes, and the supernatant was collected. Finally, EVs were pelleted by centrifugation at 14,000*g* at 4°C for 90 minutes and suspended in HBSS. Protein concentration was determined by measuring the absorbance at 205 nm using a spectrometer (Nanodrop, Mettler Toledo). EV preparations were completed with human serum albumin (0.3%) and frozen at −80°C until used. When EV extraction was not possible (manipulation of fresh tissue not possible due to the surgery schedule),

JACC: BASIC TO TRANSLATIONAL SCIENCE VOL. 9, NO. 7, 2024
JULY 2024:845-864

FIGURE 1 EVs Release in Human Pathological Valves

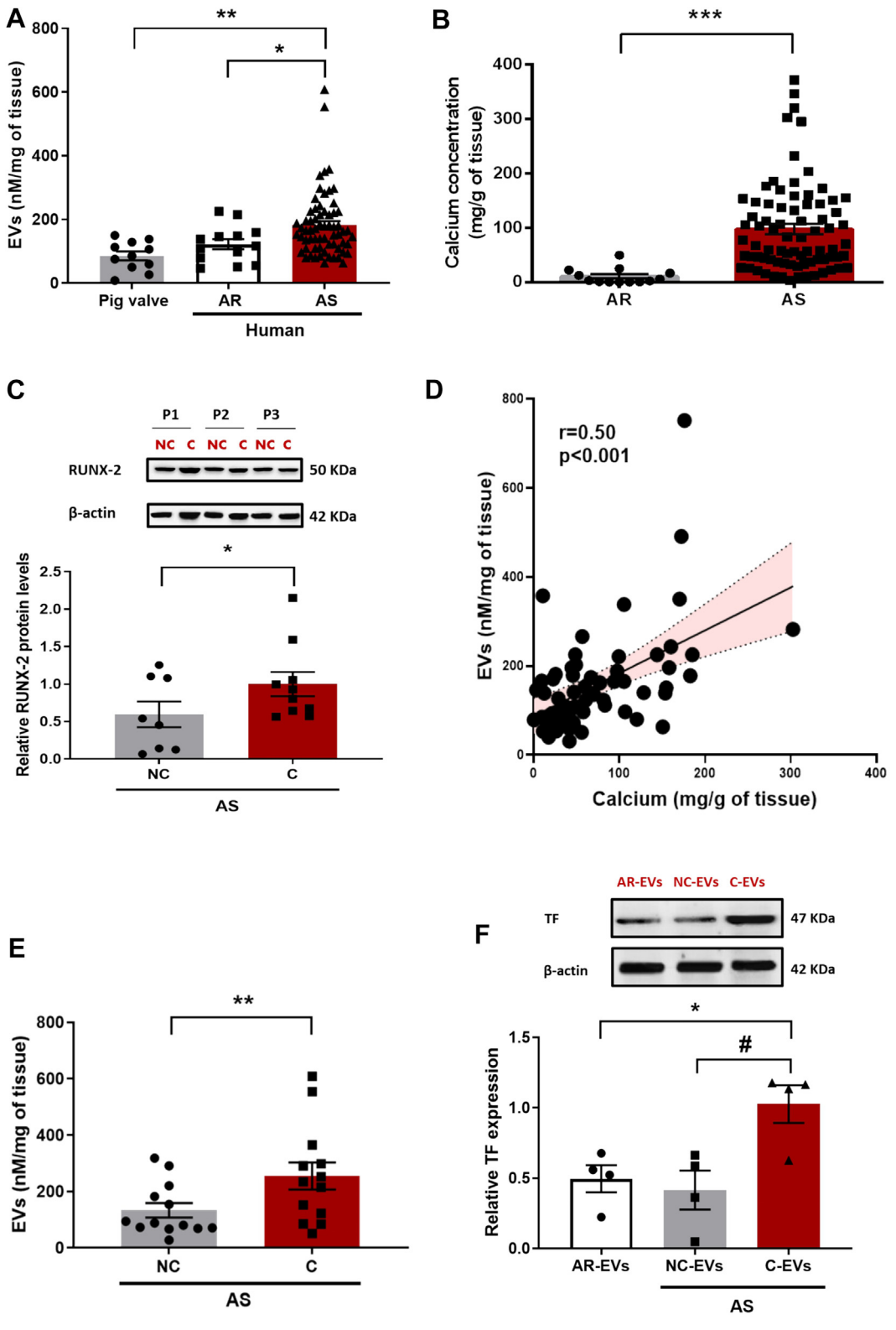

Continued on the next page

valves were used for other experimentations (histology, immunostaining) (Supplemental Figure 1). Platelets were provided by EFS (Etablissement Français du Sang) upon their extraction from healthy blood donors. Thrombin was added at a final concentration of 1 U/mL to tubes to activate the platelets. Each tube was then mixed gently and evenly, and subsequently placed in a 37°C cell incubator for 90 minutes. Dabigatran (direct thrombin inhibitor) was added for 30 minutes before the end of the stimulation period to inhibit thrombin. The suspension was centrifuged at 1,500*g* for 15 minutes at 4°C, and the supernatant was transferred to a new 2-mL tube. The supernatant was further centrifuged at 14,000*g* for 90 minutes at 4°C, and the supernatant was discarded, leaving the pellet, which contained the platelet-EVs. Erythrocytes were extracted from healthy donors and then incubated for 2 hours with phorbol 12-myristate-13-acetate (6 μmol/L). The suspension was centrifuged at 1,500*g* for 15 minutes at 4°C, and the supernatant was transferred to a new 2-mL tube. The supernatant was further centrifuged at 14,000*g* for 90 minutes at 4°C, and the supernatant was discarded, leaving the pellet, which contained the erythrocyte-EVs.

EV PROTHROMBINASE ACTIVITY QUANTIFICATION. EV prothrombinase activity measurement was performed as previously described.[8] EVs were captured onto Annexin-V–coated (prepared in the lab) microplate (Sigma, 119865001) using a microplate spectrophotometer (Molecular Devices VersaMax) set in kinetic mode. Immobilized EVs were incubated with Factor Xa (53 pmol/L, CRYOPEP, 9-HCXA-0060), Factor Va (250 pmol/L, CRYOPEP, 9-HCVA-0110), prothrombin (1.2 μmol/L, Hyphen BioMed, PP006B), and 2.2 mmol/L $CaCl_2$ in Tris buffer saline for a 10-minute incubation period at 37 C. Conversion of prothrombin to thrombin was revealed after 15 minutes by the cleavage of a specific chromogenic thrombin substrate, paranitroaniline peptide (pNA-PEP) (1.52 mmol/L, CRYOPEP, 61010216) using a microplate spectrophotometric reader set in kinetic mode, at 405 nm. Results were expressed as nanomolar phosphatidylserine equivalent (nmol/L PhtdSer eq) with reference to a standard curve constructed using liposomes of known concentration and PhtdSer eq. Identification of EV size was performed using a Particle Metrix ZetaView. Determination of EV cellular origin was performed after capture onto specific antibodies for leukocytes (CD11a), platelets (GPIb), erythrocytes (CD235), and endothelial cells (CD31). After EV incubation and washing, antibody-captured procoagulant EVs were quantified by functional prothrombinase assay.

TABLE 2 Cellular Origin and Size of EVs Extracted From Human Valves

	Aortic Stenosis	Aortic Regurgitation	*P* Value
Leukocytes, $CD11a^+$	5.9 ± 1.5 (22)	4.5 ± 2 (8)	0.61
Platelets, $GPIb^+$	1.3 ± 0.50*** (22)	0.18 ± 0.18 (8)	<0.001
Erythrocytes, $CD235a^+$	1.6 ± 0.57*** (22)	0.18 ± 0.18 (8)	<0.001
ECs, $CD31^+$	2.4 ± 0.48 (22)	2.7 ± 0.87 (8)	0.73
Activated ECs, $CD105^+$	25.5 ± 3.5 (22)	26.5 ± 3.1 (8)	0.08
Size, nm	145.2 ± 3.3 (8)	149.3 ± 3.2 (7)	0.82
Prothrombinase activity, nmol/L/mg of tissue	182.3 ± 12.5* (65)	122 ± 16 (13)	0.03

Values are mean ± SEM (n). Extracellular vesicles (EVs) cell origin was determined after capture onto specific antibodies and quantification by prothrombinase assay. Data are of n = 22 (aortic stenosis), n = 8 (aortic regurgitation) for immunocapture experiments, n = 8 (aortic stenosis), n = 7 (aortic regurgitation) for EVs sizing experiments, and n = 65 (aortic stenosis), n = 13 (aortic regurgitation) for prothrombinase activity. The between-group values were compared using Student's unpaired *t*-test. *<0.05; ***<0.001.

ECs = endothelial cells.

STATISTICAL ANALYSIS. Main clinical and echocardiographic characteristics are presented as counts and percentages for categorical variables, and medians with 25th-75th percentiles (Q1-Q3) for continuous variables. Categorical variables were compared using the chi-square or Fisher's exact test (expected cell count <5), whereas continuous variables were compared using the Wilcoxon rank-sum test.

FIGURE 1 Continued

(A) Shedding of extracellular vesicles (EVs) (nmol/L eTPES/mg of tissue) in human aortic stenosis (AS) valves (n = 65) compared with human aortic regurgitation (AR) valves (n = 13) and porcine healthy valves (n = 11). Data are expressed as mean ± SEM; *$P < 0.05$, **$P < 0.01$, vs AS (multiple Student's unpaired *t*-tests). (B) Calcium concentration in AS valves (n = 78) compared with AR valves (n = 13). Data are expressed as mean ± SEM; ***$P < 0.001$ vs AR (Student's unpaired *t*-test). (C) RUNX-2 protein expression in the calcified (C) vs the noncalcified (NC) part of the AS valve (n = 8). Data are expressed as mean ± SEM; *$P < 0.05$ vs the C part (Student's paired *t*-test). (D) Correlation between shedding of EVs (nmol/L eqPS/mg of tissue) and calcium concentration (mg/tissue) of AS valves (n = 62) (Pearson's correlation). (E) Shedding of EVs (nmol/L eqPS/mg of tissue) in the C vs the NC part of the valve (n = 13). Data are expressed as mean ± SEM; **$P < 0.01$ vs the C part (Student's paired *t*-test). (F) TF protein expression in EVs extracted from the C part compared with EVs from the NC part of AS valve and AR. Results represent blots (upper), and corresponding cumulative data (lower). Data are expressed as mean ± SEM; *$P < 0.05$ vs AR, #$P < 0.05$ vs NC. All comparisons were performed by repeated measures analysis of variance followed by Tukey's post hoc analyses.

FIGURE 2 Oxidative Stress in the Human Pathological Valves

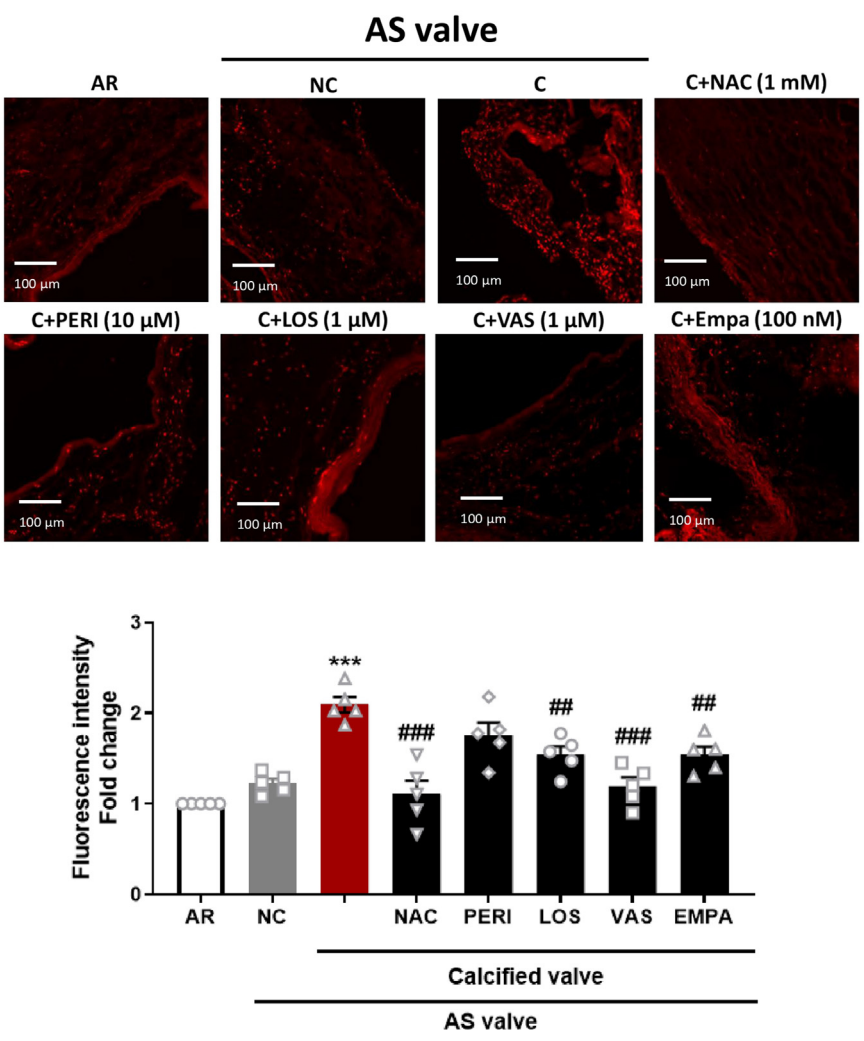

AR valves, and calcified and noncalcified segments of AS valves were exposed to dihydroethidium staining by confocal microscopy (n = 5). The calcified segments of the AS valves were incubated with *N*-acetylcysteine (NAC) (1 mmol/L) for 2 hours and either with VAS-2870 (1 μmol/L), losartan (LOS) (1 μmol/L), perindoprilat (PERI) (10 μmol/L), or empagliflozin (EMPA) (100 nmol/L) for 30 minutes before the subsequent determination of dihydroethidium staining by confocal microscope. Results are shown as micrography of dihydroethidium staining (upper and left) and corresponding cumulative data (lower and right). Data are expressed as mean ± SEM of 5 different patients; $^{***}P < 0.001$ vs AR and $^{\#\#}P < 0.01$, $^{\#\#\#}P < 0.001$ vs the C part. All comparisons were performed by 1-way analysis of variance followed by Tukey's post hoc analyses. Abbreviations as in Figure 1.

Valve characteristics are presented in the figures as the mean ± SEM based on n different experiments or as boxplots. Comparisons between or within 2 groups used the Student's unpaired or paired *t*-test, respectively. Comparisons among >2 groups used an analysis of variance followed by Tukey's post hoc test for multiple pairwise comparisons. The normality of the distribution was determined using Shapiro-Wilk normality test. Linear regression was used to compare 2 continuous variables with Pearson's correlation presented. Statistical analyses were performed using GraphPad Prism (version 7.0 for Windows, GraphPad Software), and a P value <0.05 was considered statistically significant.

FIGURE 3 Effect of AS-EVs on VECs

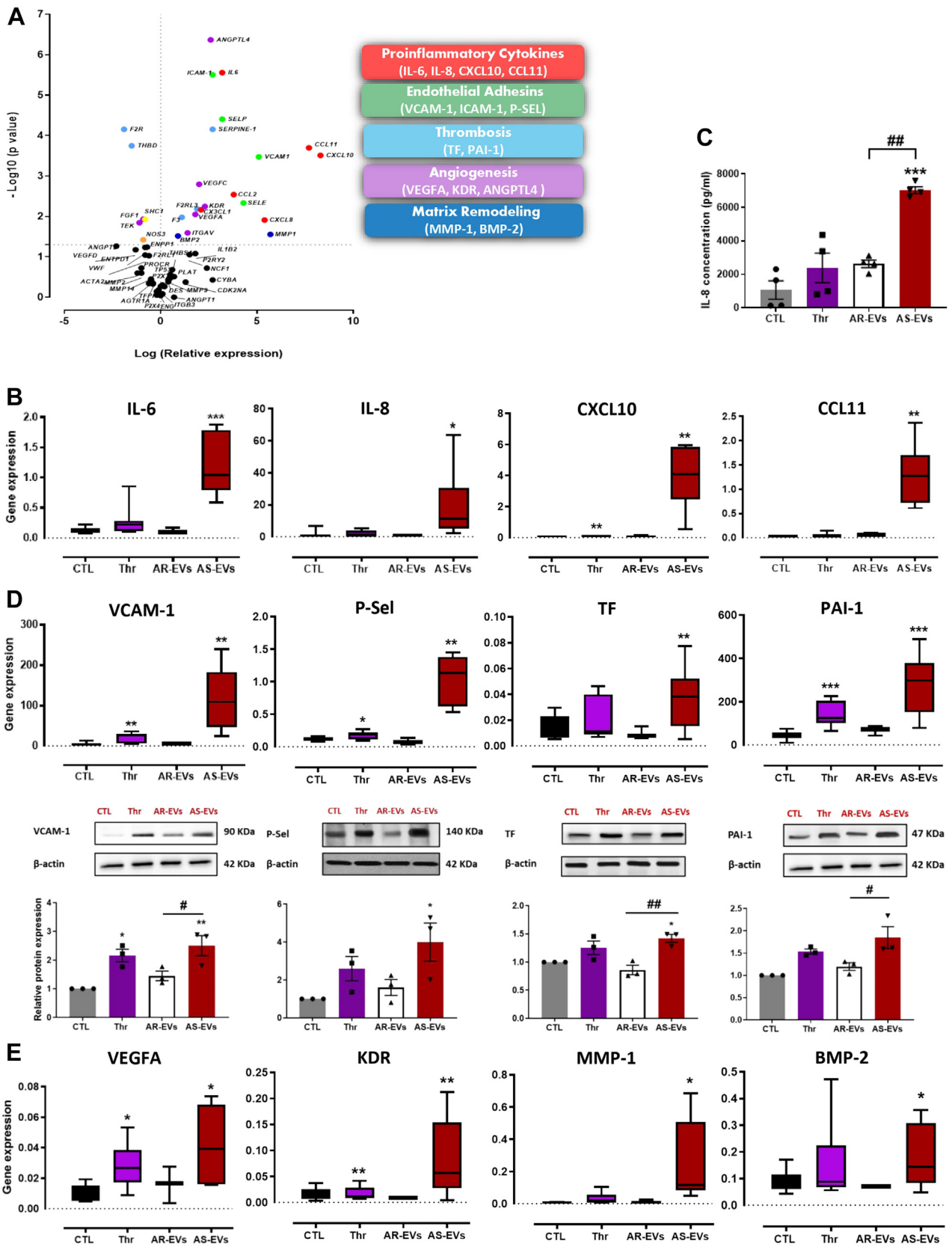

Continued on the next page

JACC: BASIC TO TRANSLATIONAL SCIENCE VOL. 9, NO. 7, 2024
JULY 2024:845–864

RESULTS

The baseline characteristics of the 105 patients enrolled in the present study are listed in Table 1.

ENHANCED PROCOAGULANT EV GENERATION AND TISSUE ACTIVATION IN CALCIFIED VALVES FROM PATIENTS WITH AS: ROLE OF THE AT1R/NADPH OXIDASES/SGLT2 PRO-OXIDANT PATHWAY. Enrichment in procoagulant EVs, as determined by prothrombinase activity, could be evidenced within AS valves with respect to AR valves or healthy porcine valves (Figure 1A). The characterization of AS-EVs indicated that they had a size of 145.2 ± 3.4 nm and originated from endothelial cells, platelets, erythrocytes, and leukocytes (Table 2). As expected, calcium concentration of AS valves was markedly increased compared with AR valves (Figure 1B). In AS valves, the protein expression of Runt-related transcription factor 2 (RUNX-2), a key factor of osteoblastic differentiation, was significantly increased in the calcified part of the valve compared with the noncalcified part (Figure 1C).

Significant correlation between EVs levels and calcium content could be established in AS valves ($r = 0.50$: $P < 0.001$) (Figure 1D). By contrast, no relationship between EV valve content, and clinical and echocardiographic characteristics could be demonstrated (Supplemental Table 1). When deciphering calcified vs noncalcified segments of the valves, additional enrichment in EVs could be evidenced in the calcified part of the valve (Figure 1E). Figure 1F shows enhanced tissue factor (TF) expression in EVs extracted from calcified segments of AS valves with respect to EVs from noncalcified segments or EVs from AR valves.

To gain a better phenotypical characterization, hematoxylin and eosin staining was performed to delineate calcified and noncalcified parts of the AS valves. In the calcified part of the AS valve, increased immunofluorescent staining of the proliferation marker PCNA, CD68 (monocytes), and SGLT2 was observed, whereas that of endothelial NO synthase (eNOS), a surrogate marker of endothelial health, was decreased (Supplemental Figure 2). Calcified parts of the AS valves also showed a higher level of oxidative stress compared with noncalcified parts of AS valves and with AR valves (Figure 2). The elevated level of oxidative stress was significantly reduced by the antioxidant *N*-acetylcysteine (NAC), the NADPH oxidase inhibitor VAS-2780, the AT1R antagonist losartan, and the SGLT2 inhibitor empagliflozin, suggesting the involvement of the AT1R/NADPH oxidases/SGLT2 pro-oxidant pathway (Figure 2). Conversely, no impact of the angiotensin-converting enzyme (ACE) inhibitor perindoprilat on oxidative stress in calcified AS valves could be established (Figure 2).

Next, the expression level of several components of the AT1R/NADPH oxidases/SGLT2 pathway and of thrombotic responses was determined. With respect to noncalcified parts, increased protein expression of ACE, $p67^{phox}$ NADPH oxidase subunit, SGLT2, and of cytoadhesins (VCAM-1, ICAM-1), inflammatory markers (p-p65 NF-κB, COX-1, COX-2), and various molecules involved in the thrombosis process such as TF, thrombomodulin (TM), and plasminogen activator inhibitor-1 (PAI-1) was observed in calcified AS valves (Supplemental Figure 3). Conversely, eNOS expression was significantly decreased in the calcified AS valves, consistent with immunofluorescent observations (Supplemental Figure 3).

AS-EVs PROMOTE VEC ACTIVATION LEADING TO IMPAIRED eNOS-NO/REACTIVE OXYGEN SPECIES BALANCE, PROADHESIVE AND PROCOAGULANT RESPONSES THAT ARE MEDIATED BY THE AT1R/NADPH OXIDASES/SGLT2 PRO-OXIDANT PATHWAY. CONTRIBUTION OF PLATELET-DERIVED EVs. To investigate the possible impact of EVs trapped in human AS valves on endothelial cells, cultured porcine VECs at first passage were exposed to EVs at a concentration similar to that observed in the peripheral circulation (10 nmol/L),[8] or to thrombin (1 U/mL), a potent blood-derived activator of endothelial cells, for 24 hours.

Results displayed in the volcano plot demonstrated a strong up-regulation of several genes encoding proinflammatory cytokines (IL-6, IL-8, CXCL10,

FIGURE 3 Continued

(A) Volcano plot showing the distribution of relative gene expression (log of fold changes) and *P* values (log10) in VECs stimulated with AS-EVs compared with control cells (CTL). (B) Boxplots showing the gene expression of IL-6, IL-8, CXCL10, and CCL11, in VECs treated with thrombin (Thr), AS-EVs, and AR-EVs. (C) Enzyme-linked immunosorbent assay showing an increase in IL-8 secretion in the supernatant of AS-EV-treated valvular interstitial cells (VECs). (D) Boxplots showing gene expression and respective blots showing protein expression of VCAM-1, P-SEL, TF, and PAI-1 in VECs treated with Thr, AS-EVs, and AR-EVs. (E) Boxplots showing the gene expression of VEGFA, KDR, MMP-1, and BMP-2 in VECs treated with Thr, AR-EVs, and AR-EVs. Data are expressed as mean ± SEM on experiments performed on 3 to 6 different cultures; $^{*}P < 0.05$, $^{**}P < 0.01$, $^{***}P < 0.001$ vs CTL and $^{\#\#}P < 0.01$, $^{\#\#\#}P < 0.001$ vs AS-EVs. Comparisons were performed by 1-way analysis of variance followed by Tukey's post hoc analyses and multiple Student's paired *t*-tests. Abbreviations as in Figure 1.

FIGURE 4 ROS Formation in VECs Exposed to EVs

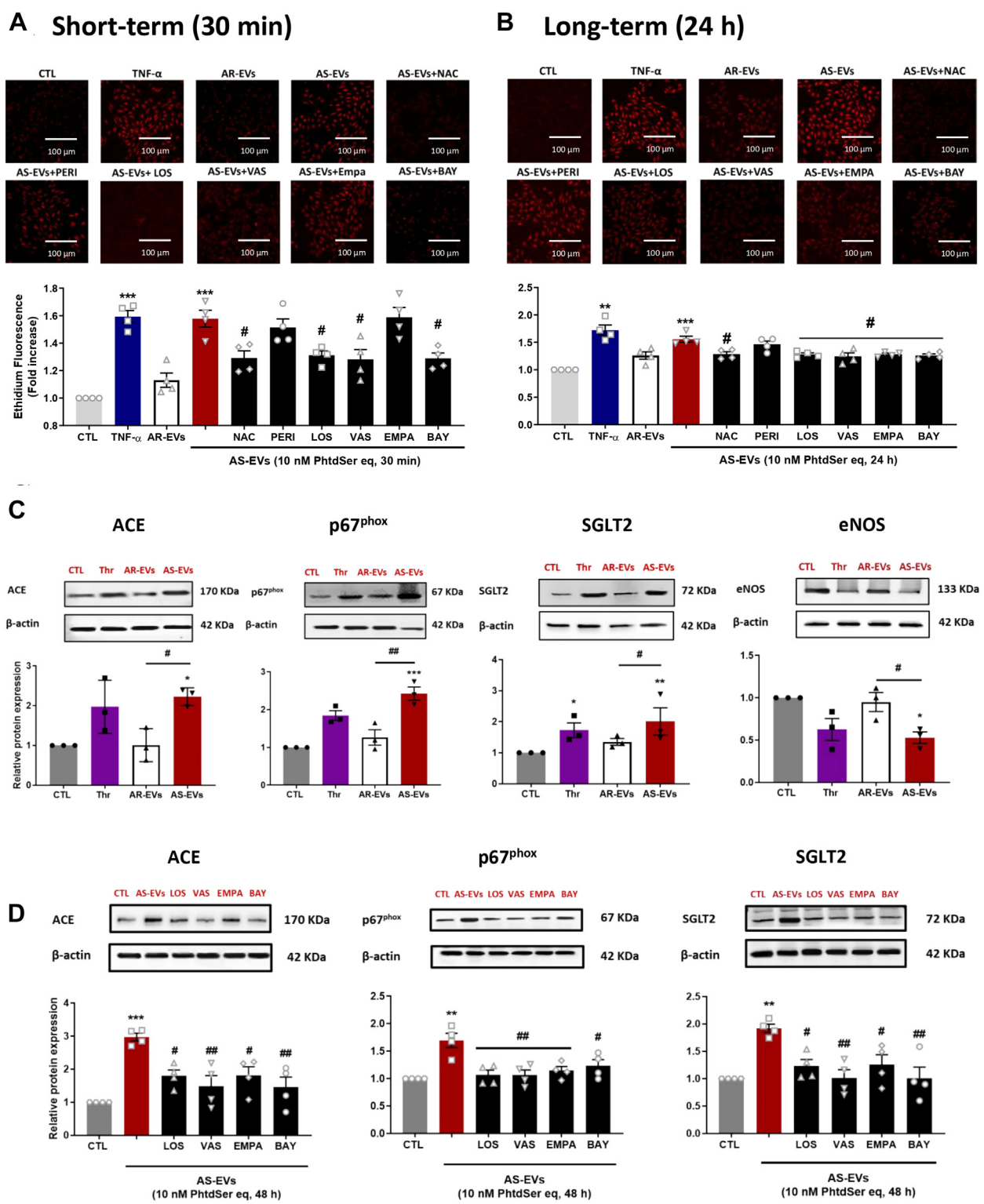

Continued on the next page

CCL11) in VECs exposed to AS-EVs (Figures 3A and 3B). IL-8 concentration was markedly increased in the supernatant of VECs when exposed to AS-EVs with respect to AR-EVs or thrombin (Figure 3C). Moreover, exposure of VECs to AS-EVs caused a significant increase in the expression of adhesion molecules (VCAM-1, ICAM-1, P-SEL) and prothrombotic molecules (TF, PAI-1) at both the gene and protein expression levels (Figure 3D, Supplemental Figure 4A), and also of proangiogenic molecules (KDR, VEGFA, ANGPTL4) and matrix remodeling molecules (MMP-1, BMP-2) at the gene level (Figure 3E, Supplemental Figure 4B). In contrast to AS-EVs, AR-EVs and thrombin had either no effect or caused only a small, but significant, expression of the target genes in VECs (Figure 3, Supplemental Figure 4).

Because proinflammatory cytokines stimulate the formation of reactive oxygen species in endothelial cells,[9] we evaluated the ability of AS-EVs to induce oxidative stress in VECs. Exposure of VECs to AS-EVs increased the level of oxidative stress within 30 minutes and the stimulatory effect persisted up to 24 hours (Figures 4A and 4B). The pro-oxidant effect of AS-EVs was similar to that observed with tumor necrosis factor (TNF)-α, a major proinflammatory cytokine (Figures 4A and 4B). Conversely, no impact of AR-EVs on short-term and long-term oxidative stress could be demonstrated (Figures 4A and 4B). Both the short and sustained pro-oxidant responses to AS-EVs were inhibited by *N*-acetylcysteine, losartan, VAS-2870, and by the NF-κB inhibitor, BAY 11-7082 (Figures 4A and 4B). In addition, although empagliflozin did not affect the AS-EV-induced short-term pro-oxidant response, it markedly reduced the sustained one (Figures 4A and 4B). Altogether, these findings indicate that the AS-EV-induced early pro-oxidant response is mediated by the AT1R/NADPH oxidases pathway and, thereafter SGLT2, that further contributes to perpetuate the activator signal most likely subsequent to its enhanced expression. Indeed, exposure of VECs to AS-EVs for 48 hours increased the low expression of SGLT2 protein observed in control cells, and this effect was associated with enhanced protein levels of ACE and the $p67^{phox}$ NADPH oxidase subunit, whereas no such effects were observed with AR-EVs (Figure 4C). In addition, AS-EVs, but not AR-EVs, significantly down-regulated the expression of eNOS in VECs (Figure 4C). Losartan, VAS-2870, empagliflozin, and BAY 11-7082 significantly blunted AS-EV-mediated enhanced protein levels of ACE, $p67^{phox}$, and SGLT2 (Figure 4D).

We further investigated the pathway by which AS-EVs induced the pro-oxidant response. VECs were induced with AS-EVs in the presence of toll-like receptor 2 (TLR2) antagonist, toll-like receptor 4 (TLR4) inhibitor, key innate immunity receptors, and RAGE (receptor for advanced glycation products) antagonist. The pro-oxidant responses to AS-EVs were significantly reduced by TLR2 antagonist, TLR4 inhibitor, and the combination of both. However, RAGE antagonist had no effect on the pro-oxidant response induced by AS-EVs (Figure 5A). Thus, these findings suggest that AS-EVs are interacting with VECs through TLR2 and TLR4, eventually mediating the AT1R/NADPH oxidases/SGLT2 pathway (Figure 5A).

Because the characterization of AS-EVs and AR-EVs has indicated significant contribution of platelet-EVs and red blood cell (RBC)-EVs in AS-EV–mediated signaling (Table 2), we explored separately the effect of platelet-EVs and RBC-EVs on VECs dysfunction. The pro-oxidant effect of platelet-derived EVs was similar to that observed with TNF-α and AS-EVs (Figure 5B). Conversely, no impact of RBC-derived EVs on oxidative stress could be demonstrated (Figure 5C). The pro-oxidant responses to platelet-EVs were inhibited by *N*-acetylcysteine, losartan, VAS-2870, empagliflozin, TLR2 antagonist, TLR4 inhibitor (Figure 5B). However, RAGE antagonist had no effect on the pro-oxidant response induced by platelet-derived EVs (Figure 5B). AS-EVs depleted from platelet-derived EVs and RBC-derived EVs demonstrated a significant 1.3-fold increase in the induced oxidative stress, which is lower than that

FIGURE 4 Continued

(A and B) Levels of oxidative stress as measured by ethidium fluorescence in VECs exposed to EVs (10 nmol/L phosphatidylserine equivalent [PhtdSer eq]) and TNF-α (10 ng/mL) after 30 minutes and 24 hours. NAC (1 μmol/L), perindoprilat (10 μmol/L), LOS (1 μmol/L), VAS-2870 (1 mmol/L), EMPA (100 nmol/L), and BAY 11-7082 (3.5 μmol/L) were used to reduce the pro-oxidant responses to AS-EVs. (C) VECs exposed for 48 hours to EVs (10 nmol/L PhtdSer eq) and thrombin (1 U/mL) and either LOS (1 μmol/L), VAS-2870 (1 μmol/L), EMPA (100 nmol/L), or BAY 11-7082 (3.5 μmol/L) for 30 minutes before the addition of AS-EVs and the subsequent determination of the expression level of target proteins by Western blot analysis. Data are expressed as mean ± SEM on 3 to 4 different cultures; $^{*}P < 0.05$, $^{**}P < 0.01$, $^{***}P < 0.001$ vs CTL and $^{\#}P < 0.05$, $^{\#\#}P < 0.01$ vs AS-EVs (A, B, and D) vs AR-EVs (C). All comparisons were performed using 1-way analysis of variance followed by Tukey's post hoc analyses. ROS = reactive oxygen species; other abbreviations as in Figures 1 to 3.

FIGURE 5 **Oxidative Stress in VECs Exposed to Platelet-EVs and RBC-EVs**

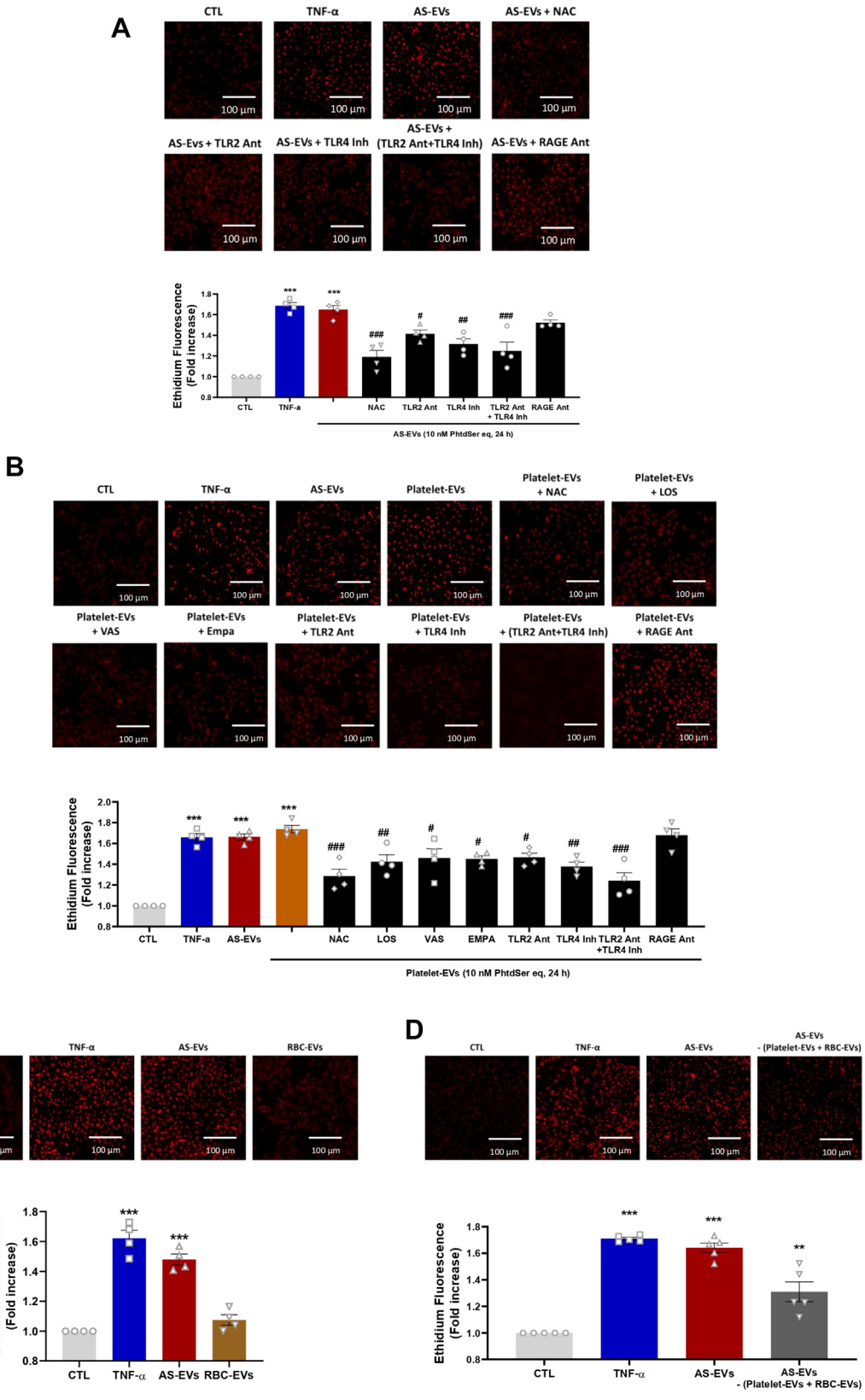

Continued on the next page

JACC: BASIC TO TRANSLATIONAL SCIENCE VOL. 9, NO. 7, 2024
JULY 2024:845–864

induced by all components of AS-EVs (1.6-fold increase) (Figure 5D). Altogether, these data suggest that part of the pro-oxidant effect of AS-EVs on VECs is mediated by platelet-derived EVs.

Because AS-EVs promoted oxidative stress associated with eNOS down-regulation in VECs, the impact on the formation of NO, a major vasoprotective factor, was evaluated. AS-EVs reduced the bradykinin-stimulated formation of NO without affecting the basal formation of NO. Such effect was prevented by *N*-acetylcysteine indicating a pro-oxidant-dependent event (Figure 6A). In addition, the blunted formation of NO was also prevented by inhibition of the AT1R, NADPH oxidases, SGLT2, and NF-κB, and also by the TNF-α neutralizing antibody infliximab, whereas perindoprilat was inactive (Figure 6B). Thus, the AS-EV-induced blunted endothelial formation of NO is mediated by the AT1R/NADPH oxidases/SGLT2 pro-oxidant pathway and also by the proinflammatory cytokine TNF-α.

AS-EV–INDUCED VECs ACTIVATION INVOLVES NF-κB ACTIVATION VIA THE AT1R/NADPH OXIDASES/SGLT2 PATHWAY AND THE MAPKs PATHWAY. Because a previous study has shown that NF-κB, a redox-sensitive transcription factor, contributes to regulate SGLT2 gene expression,[10] the activation of NF-κB was evaluated. AS-EVs, but not AR-EVs, caused the phosphorylation of p65 NF-κB in VECs, indicating its activation (Figure 7A). AS-EVs' mediated effect on p65 NF-κB phosphorylation was prevented by losartan, VAS-2870, empagliflozin, and BAY 11-7082, indicating a major role of the AT1R/NADPH oxidases/SGLT2 pathway (Figure 7B). Furthermore, the role of redox-sensitive MAPKs known to cause activation of NF-κB by phosphorylation followed by its nuclear translocation to regulate the expression of target genes, including those encoding components of the angiotensin system, inflammatory molecules, prothrombotic molecules, and SGLT2,[10] was investigated. AS-EVs induced within 30 minutes the phosphorylation of p38 MAPK, extracellular signal-regulated kinases (ERK1/2), and c-jun N-terminal kinase (JNK) in VECs in a time-dependent manner, which persisted up to 2 hours (Figure 7C). Inhibition of either p38 MAP kinases, ERK1/2, or JNK significantly blunted the AS-EV-induced NF-κB phosphorylation (Figure 7D). Altogether, these findings underscore that AS-EV-induced VECs activation involves NF-κB subsequent to the stimulation of the AT1R/NADPH oxidases/SGLT2 pathway and MAPKs pathway.

AS-EVs PROMOTE INFLAMMATORY CELL RECRUITMENT AND THROMBIN GENERATION ON VECs. To emphasize the link between VEC dysfunction, recruitment of inflammatory cells, and thrombogenicity, we examined the impact of AS-EVs on monocytes adhesion on VECs and the procoagulant activity. Exposure of VECs to AS-EVs caused an increased adhesion of THP1 cells (a monocytic human cell line) and an enhanced generation of thrombin that was dependent on surface TF (Figure 8). Similar effects were also observed in VECs exposed to TNF-α (Figure 8). The AS-EV-induced enhanced adhesion of THP1 cells was abolished by losartan, VAS-2870, and empagliflozin, and by the inhibition of NF-κB (Figure 8A).

The characterization of the AS-EV-induced surface procoagulant activity on VECs indicated a pronounced inhibition by the direct thrombin inhibitor dabigatran and also a slight, but significant, inhibition by the direct Factor Xa inhibitor rivaroxaban, indicating that it is mostly mediated by thrombin (Figure 8B). Significant inhibition by losartan, VAS-2870, empagliflozin, and NF-κB inhibitors could also be demonstrated (Figure 8B). In sum, these data underline that AS-EVs induced proadhesive and procoagulant responses on the VEC surface through the AT1R/NADPH oxidases/SGLT2 pathway.

DISCUSSION

The major findings of this study indicate that human aortic calcified valves constitute an important

FIGURE 5 Continued

(A) Levels of oxidative stress as measured by ethidium fluorescence in VECs exposed to AS-EVs (10 nmol/L PhtdSer eq) and TNF-α (10 ng/mL) after 24 hours. NAC (1 mmol/L), TLR2 antagonist (Ant) (100 μmol/L), TLR4 inhibitor (Inh) (10 μmol/L), and RAGE antagonist (1 mmol/L) were used to reduce the pro-oxidant responses to AS-EVs. (B) VECs exposed to platelet-EVs (10 nmol/L PhtdSer eq) and TNF-α (10 ng/mL) after 24 hours. NAC (1 mmol/L), LOS (1 μmol/L), VAS-2870 (1 μmol/L), EMPA (100 nmol/L), TLR2 antagonist (100 μmol/L), TLR4 inhibitor (10 μmol/L), and RAGE antagonist (1 mmol/L) were used to reduce the pro-oxidant responses to platelet-EVs. (C and D) VECs exposed to red blood cell (RBC)-EVs and Depleted-EVs (10 nmol/L PhtdSer eq) and TNF-α (10 ng/mL) after 24 hours. Data are expressed as mean ± SEM of 4 different cultures; $^{*}P < 0.05$, $^{**}P < 0.01$, $^{***}P < 0.001$ vs CTL and $^{\#}P < 0.05$, $^{\#\#}P < 0.01$, $^{\#\#\#}P < 0.001$ vs AS-EVs (A) and vs platelet-EVs (B). All comparisons were performed using 1-way analysis of variance followed by Tukey's post hoc analyses. Abbreviations as in Figures 1 to 4.

FIGURE 6 **NO Formation in VECs Exposed to AS-EVs**

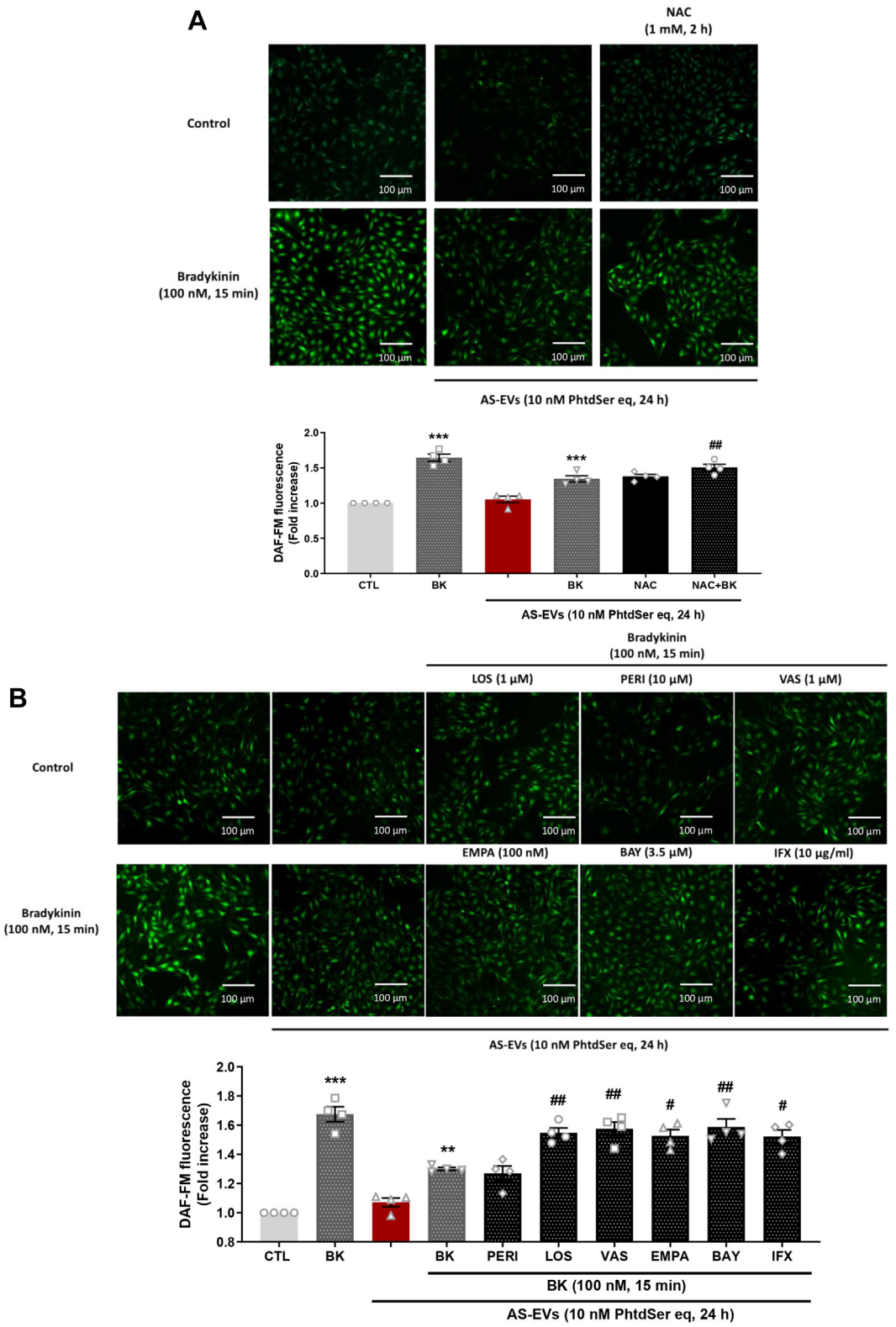

Continued on the next page

JACC: BASIC TO TRANSLATIONAL SCIENCE VOL. 9, NO. 7, 2024
JULY 2024:845–864

reservoir of thrombotic material, including procoagulant cell-derived EVs. Confined within the native valve, AS-EVs act as a potent biological agonist and transform VECs into a prothrombotic, proadhesive, and proinflammatory surface that recruits inflammatory cells and promotes thrombogenicity. These data demonstrate that AS-EVs trigger up-regulation of various proteins, including SGLT2 in VECs via the AT1R/NADPH oxidases/SGLT2 pathway, which in turn, effectively promote valvular endothelial cells dysfunction in a redox-sensitive manner.

DEGENERATIVE PHENOTYPE EXPRESSED BY HUMAN STENOTIC CALCIFIED VALVES. Although previously considered as a passive degenerative process, numerous studies have depicted AS pathogenesis as a complex interplay between the hemostasis system and the valve. This interplay triggers endothelial dysfunction, thrombosis, inflammation, fibrosis, and calcification.[3] Consistent with this paradigm, we have demonstrated the importance of the inflammatory process and endothelial damage, as shown by enhanced monocytic staining (CD68) and the expression of cytoadhesins markers VCAM-1 and ICAM-1 (leukocyte-adhesion molecules). This enhanced expression contrasts with the down-regulation of eNOS, a marker of endothelial health, in the calcified portion of the human AS valve. The significance of the inflammatory process in valvular injuries was suggested by the qualitative occurrence of infiltrating macrophages, and oxidative stress in the extent of the calcification burden, in line with previous observations that have underscored higher ^{18}F-fluorodeoxyglucose uptake, a glucose analogue captured by inflammatory cells, on positron emission tomography in patients with severe AS.[11] Other features of the calcified portion of AS included up-regulation of protein expression, including ACE, $p67^{phox}$ (NADPH oxidase subunit), p-p65 NF-κB, SGLT2, and cytoadhesins, and down-regulation of eNOS.

VALVE THROMBOGENICITY. Besides the significance of inflammatory infiltration, we demonstrated that human calcified stenotic valve constitutes a potent reservoir of thrombotic material, including procoagulant EVs, TF, and PAI-1. Pioneering works have stressed that thrombosis occurs on the aortic valve surface,[12] and they have pointed to a potential link between AS, turbulent blood flow on the native valve surface, and thrombosis. A recent Danish nationwide cohort study has shown that AS is independently associated with an increased absolute risk of ischemic stroke, even after adjusting for significant cofounding factors, such as age or atrial fibrillation. In this large cohort study, the observed decrease in the absolute risk of ischemic stroke after SAVR suggests that the native valve may act as a prothrombotic reservoir, promoting clot formation and subsequent embolism.[13] The potential contribution of the native valve, which is entrapped by the bioprosthetic valve during TAVR, has garnered interest as a possible factor in the development of leaflet thrombosis or valvular dysfunction.[4,5,14,15]

EXTRACELLULAR VESICLES AND AORTIC STENOSIS. Pioneering work from Diehl et al[16] emphasized the association of AS with the release of platelet-, leukocyte-, and endothelial cell-derived EVs[16] into the bloodstream. The release of these vesicles may be a potential consequence of altered shear stress and inflammation. The findings from these studies have provided evidence to support the theory that shear stress induced by AS initiates a vicious cycle that promotes the generation of platelet-derived EVs, the activation of monocytes, and the subsequent release of leukocyte-derived EVs. Over the course of AS, the loss of laminar shear stress, along with oxidative stress, endothelial injury, and inflammation, are potent factors that induce the shedding of EVs by VECs, macrophages, and valvular interstitial cells (VICs). Another study suggested that the restoration of normal rheology after TAVR is associated with improved endothelial function and a decrease in endothelial-derived EV levels.[17] In addition to the noxious effects of circulating EVs, there has been a growing interest in the presence of an intratissular pool of EVs trapped within the valve and acting as important mediators of cardiovascular calcification.[18]

FIGURE 6 Continued

(A) VECs studied at passage 1 demonstrated down-regulation of bradykinin-stimulated nitric oxide (NO) formation as assessed by DAF-FM in response to AS-EVs (10 nmol/L PhtdSer eq, 24 hours). (A and B) NAC (1 mmol/L), LOS (1 μmol/L), VAS-2870 (1 μmol/L), EMPA (100 nmol/L), and BAY 11-7082 (3.5 μmol/L) preserved bradykinin-stimulated NO formation. Data are expressed as mean ± SEM on experiments performed on 4 different cultures; $^{***}P < 0.001$ vs control CTL, $^{\#}P < 0.05$, $^{\#\#}P < 0.01$, $^{\#\#\#}P < 0.001$ vs AS-EVs + bradykinin. All comparisons were performed using 1-way analysis of variance followed by Tukey's post hoc analyses. Abbreviations as in Figures 1 to 4.

FIGURE 7 **AS-EVs Activate the MAPK Pathways and Phosphorylate NF-κ B**

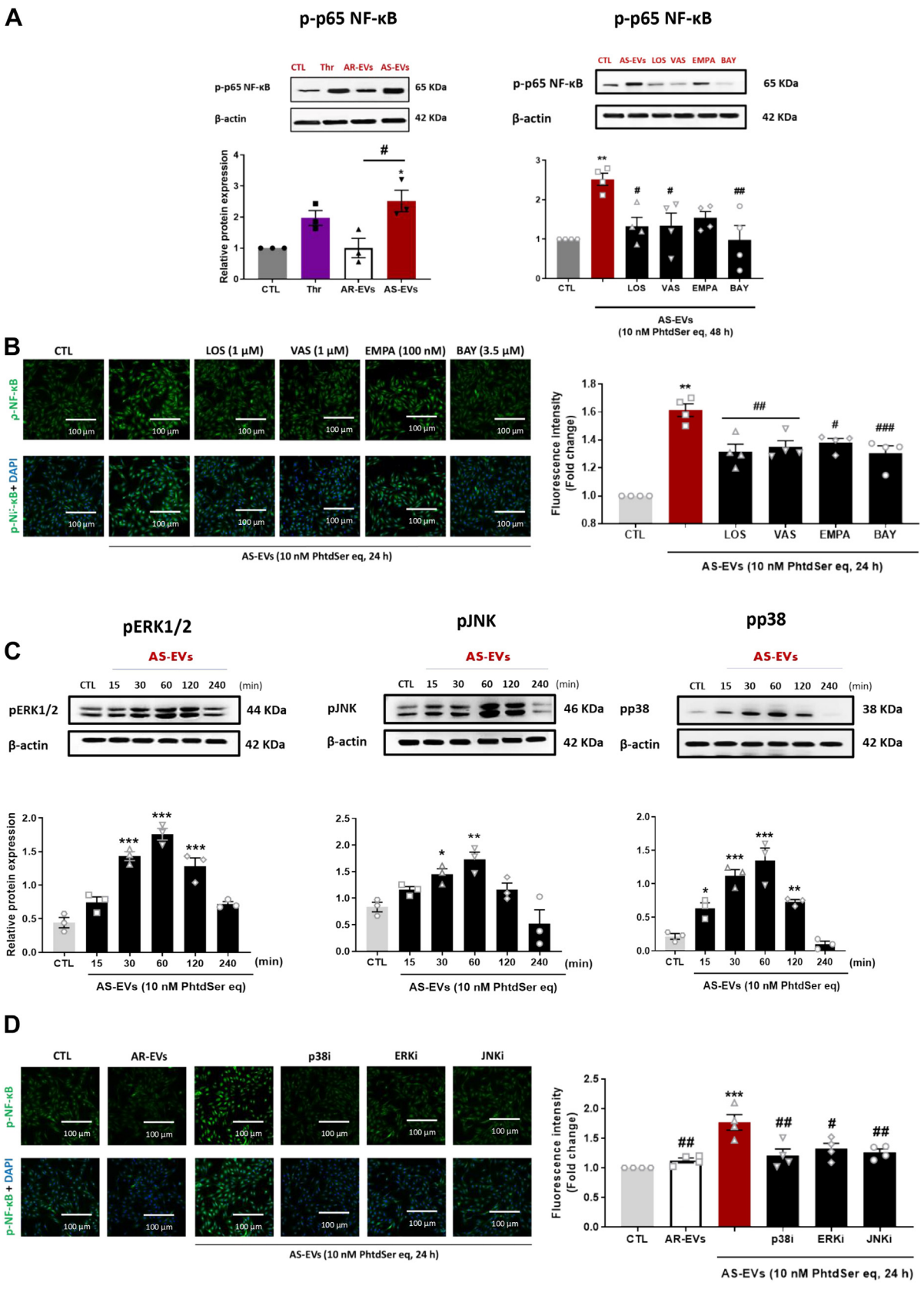

Continued on the next page

JACC: BASIC TO TRANSLATIONAL SCIENCE VOL. 9, NO. 7, 2024
JULY 2024:845–864

This pool of EVs is considered as a possible link between: 1) persistent aortic valve activity; 2) thrombotic events; and 3) valve dysfunction after TAVR.[18]

Although it was initially considered a passive, inert material, we have demonstrated significant enrichment of procoagulant EVs in the AS valve, particularly within the calcified portion. Furthermore, we observed a correlation between the content of valvular EVs and the extent of calcification, indicating that EVs may play an active role in the calcification process. Additionally, our study demonstrates that AS-EVs and thrombin induced the overexpression of BMP-2, a key mechanism involved in the propagation phase of AS and osteoblastic differentiation (**Figure 3E**).[19] Previous work has established that mechanical strain within the valve induced blebbing and the production of mineralized EVs by VICs through the RhoA/ROCK-dependent mechanism.[20] This process contributes to the entrainment of calcification of the aortic valve.

In addition to EVs' role in the calcification process, our data provide evidence that EVs trapped within the native valve act as efficient biological shuttles that tightly regulate valvular endothelial phenotype. At concentrations achieved in human clinical settings, AS-EVs transform VECs into a pro-oxidant, prothrombotic, proinflammatory, proangiogenic, and proremodeling surface. Significant contribution of platelet-derived EVs could be demonstrated in line with previous studies demonstrating an important role of platelet activation in AS progression.[3] Functional relevance of AS-EV–mediated VECs activation was underlined by the increased recruitment of inflammatory cells at the VEC's surface—a prerequisite for valve dysfunction and enhanced thrombin generation. Furthermore, AS-EVs caused a down-regulation of the protein expression of eNOS, along with reduced bradykinin-stimulated formation of NO as a surrogate marker of valvular endothelial dysfunction.[21] By contrast, AR-EVs had no deleterious impact on VECs physiology. The mechanisms underlying this discrepancy in the effectiveness of EVs remain unclear but may be related to the different vascular origins and species of EVs, as well as differences in their intrinsic pro- or antioxidant systems, or regulators of oxidative stress.

MECHANISMS OF EV-MEDIATED VEC DYSFUNCTION. In line with previous data demonstrating a key role for the innate immune receptors TLR 2 and 4 in the regulation of EV signaling,[22] angiotensin II (Ang II)-induced remodeling,[23] or inflammatory response within the aortic valve,[24] our findings highlight the importance of EV-TLR interactions in the induction of valvular dysfunction. In addition, we show that activation of the AT1R/NADPH oxidases/SGLT2 pathway, MAP kinase activation, and NF-κB phosphorylation are involved in AS-EV–mediated VEC activation, resulting in the up-regulation of genes and proteins associated with inflammation, endothelial adhesion, angiogenesis, thrombosis, and vascular remodeling. These findings are consistent with our previous observations in coronary endothelial cells.[7,25] The clinical relevance of this pathophysiological mechanism was emphasized by the up-regulation of those pathways in the calcified portion of the human valve (**Figure 2**), which mirrored the paracrine effects of AS-EVs on VECs observed ex vivo. The pro-oxidant effect of AS-EVs indicates a major role of the AT1R/NADPH oxidases, whereas the sustained signal also involves an up-regulation of SGLT2. The specific significance of the late pro-oxidant signal in driving persistent activation of ECs likely depends on a redox-sensitive NF-κB–mediated feedforward amplifying loop. This is supported by our observation that inhibition of NADPH oxidases, SGLT2, and NF-κB strongly inhibited the sustained NF-κB phosphorylation and the expression of SGLT2, ACE, $p67^{phox}$ NADPH oxidase subunit, and p-p65 NF-κB. In another study, it was found that depletion of NO in VECs, which mimics endothelial dysfunction,[26] resulted in the activation of NF-κB in VICs. Besides its key role in regulating

FIGURE 7 Continued

(A, B) Phosphorylation of NF-κB in VECs exposed to AS-EVs (10 nmol/L PhtdSer eq), thrombin (1 U/mL), and after pretreatment with either LOS (1 μmol/L), VAS-2870 (1 μmol/L), EMPA (100 nmol/L), or BAY 11-7082 (3.5 μmol/L) for 30 minutes before the addition of AS-EVs and measured by Western blot analysis and immunostaining. (C) VECs were treated with AS-EVs (10 nmol/L PhtdSer eq) for the indicated time before determination of the phosphorylation level of ERK1/2, JNK, and p38 MAPK. (D) VECs were exposed to a selective inhibitor of either p38 MAPK (p38i, SB203580, 10 μmol/L), ERK1/2 (ERKi, PD98059, 10 μmol/L) JNK (JNKi, SP600125, 10 μmol/L), for 30 minutes in the presence of AS-EVs (10 nmol/L PhtdSer eq) for 24 hours. Data are expressed as mean ± SEM of experiments performed on 3 to 4 different cultures; $^{*}P < 0.05$, $^{**}P < 0.01$, $^{***}P < 0.001$ vs control (CTL), and $^{\#}P < 0.05$, $^{\#\#}P < 0.01$ vs AS-EVs. All comparisons were performed using 1-way analysis of variance followed by Tukey's post hoc analyses. Abbreviations as in **Figures 1 to 4**.

FIGURE 8 Effect of AS-EVs on THP-1 Cell Adherence and Thrombin Generation in VECs

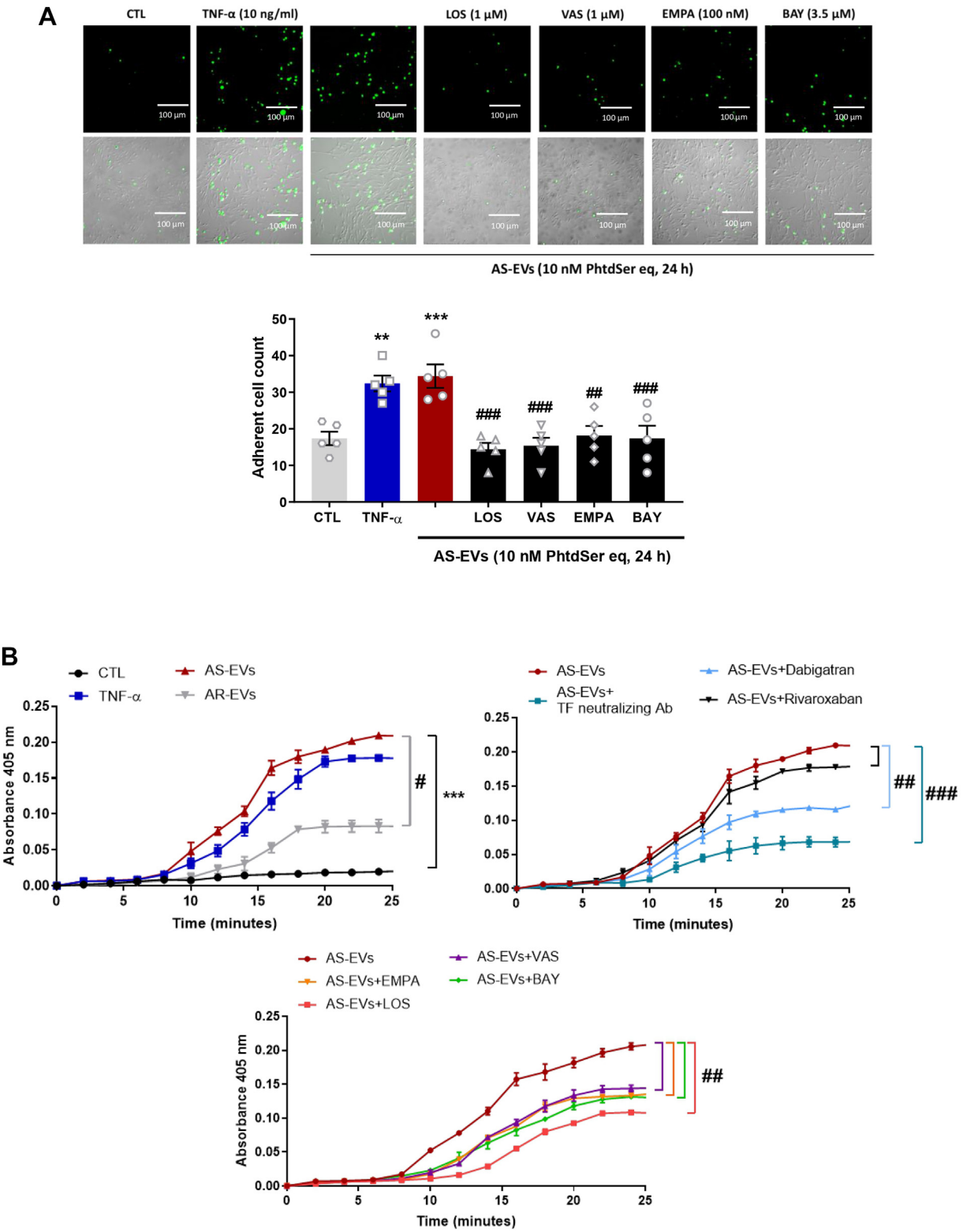

Continued on the next page

various genes involved in inflammation, cell adhesion, and thrombogenicity, NF-κB acts as a transcription factor for DPP-4, which can decrease insulin-like growth factor (IGF)-1 levels through enzymatic degradation. Subsequently, higher levels of IGF-1 lead to greater osteoblastic differentiation of VICs and valve mineralization.[1,26] Downstream targets of NF-κB also include proinflammatory cytokines IL-1β and IL-6, which have been demonstrated to promote mineralization of VICs and activate an osteogenic program.[2] Further characterization of the signal transduction pathway involved in AS-EV-induced VEC activation indicated the involvement of various redox-sensitive kinases, including p38 MAPK, JNK, and ERK1/2, as well as phosphorylation of NF-κB. Inhibitors of MAPKs blunted AS-EV–induced NF-κB phosphorylation, indicating that redox-sensitive MAPKs act upstream. Furthermore, the preventive effects of losartan, and inhibition of NADPH oxidases and SGLT2 on AS-EV-induced phosphorylation of NF-κB, suggest that AS-EVs act upstream via activation of AT1R/NADPH oxidases/SGLT2-induced oxidative stress, which triggers phosphorylation of the redox-sensitive MAPKs and NF-κB, ultimately promoting VEC activation. The translocation of phosphorylated NF-κB within the nucleus ultimately promotes inflammation and valvular calcification. A previous observation confirmed the significant role of the AKT/NF-κB/NLRP3 inflammasome pathway in aortic valve calcification.[27] Collectively, our findings reveal that human native aortic calcified valves constitute an important reservoir of procoagulant EVs that tune thrombotic and inflammatory responses in VECs.

Considering the impact of AS-EVs on the local activation of ACE, AT1R, and SGLT2, and the paramount importance of finding therapeutic approaches to curb valve disease progression, we investigated the local effect of modulating the angiotensin system along with SGLT2 inhibition. ACE/ang II receptors have been identified on valve myofibroblasts and up-regulated in AS.[28,29] Conversely, the down-regulation of ACE/angiotensin is believed to promote fibrosis, proliferation, and inflammation in AS.[30] Consistent with this paradigm, clinical data have suggested that ACE inhibition lead to a modest, but progressive, reduction in left ventricular mass in asymptomatic patients with moderate-to-severe AS compared with placebo, with a trend towards a slower progression of valvular stenosis.[31] In our study, an interaction between AS-EVs and the local angiotensin system was suggested by: 1) up-regulation of ACE expression by VECs following EV exposure; 2) short- and long-term reduction of AS-EV–mediated oxidative stress after AT1R blockade by losartan; and 3) preservation of bradykinin-induced production of NO by losartan after AS-EV exposure. Overall, these findings highlight a novel mechanism through which AS-EVs up-regulate the local angiotensin system, resulting in the redox activation of VECs and subsequent endothelial dysfunction. The ongoing ROCK-AS trial[32] will provide consistent information regarding the relevance of this pathway. This trial is analyzing valvular inflammation, calcification, lipid accumulation, and fibrosis through histological analysis of aortic valves removed in SAVR patients treated by candesartan.

An important finding of this study is the description of another marker of valvular dysfunction: the enhanced expression of SGLT2 in the calcified segments of AS. Although the pathophysiological mechanisms underlying the cardiac protective effects of sodium-glucose co-transporter 2 inhibitor (SGLT2i) have not been fully described, decreased oxidative stress and inflammation together with the regulation of immune signaling pathways are considered as potent pathways. Although the presence of SGLT2 within the cardiovascular system was questioned until recently, we have demonstrated that Ang II and EVs, which are possible mediators of endothelial damage, act as potent inducers of SGLT1 and SGLT2 expression in ECs.[25] This effect was also observed ex vivo in pathological rat arteries (ie, aortic arch, Ang

FIGURE 8 Continued

(A) VECs exposed to TNF-α (10 ng/mL) and AS-EVs (10 nmol/L PhtdSer eq) for 24 hours demonstrated increased THP-1 adherent cell count. LOS (1 μmol/L), VAS-2870 (1 μmol/L), EMPA (100 nmol/L), and BAY 11-7082 (3.5 μmol/L) exhibited diminished AS-EV–mediated THP-1 adherence. Data are expressed as mean ± SEM of experiments performed on 4 to 5 different cultures. $^{**}P < 0.01$, $^{***}P < 0.001$ vs CTL and $^{\#\#}P < 0.01$, $^{\#\#\#}P < 0.001$ vs AS-EVs (1-way analysis of variance followed by Tukey's post hoc analysis). (B) Thrombin generation was measured in VECs upon the exposure to EVs (10 nmol/L PhtdSer eq) and TNF-α (10 ng/mL) (upper left). AS-EV–mediated thrombin generation in VECs was measured after the exposure to TF neutralizing antibody (10 μg/mL), dabigatran (10 μmol/L), and rivaroxaban (10 μmol/L) (upper right), and LOS (1 μmol/L), VAS-2870 (1 μmol/L), EMPA (100 nmol/L), and BAY 11-7082 (3.5 μmol/L) (bottom). Data are expressed as mean ± SEM of experiments performed on 4 to 5 different cultures. $^{***}P < 0.001$ vs CTL and $^{\#}P < 0.05$, $^{\#\#}P < 0.01$, $^{\#\#\#}P < 0.001$ vs AS-EVs. Comparisons were performed by 1-way analysis of variance followed by Tukey's post hoc analyses and multiple Student's paired *t*-tests. Abbreviations as in **Figures 1 to 4**.

II-, and eNOS inhibitor-treated thoracic aorta vs thoracic aorta) promoting oxidative stress in the arterial wall and endothelial dysfunction.[25] In this study, we provide new evidence of AS-EVs acting as potent inducers of SGLT2 expression in VECs through sustained oxidative stress. Furthermore, we establish ex vivo that increased SGLT2 levels induce endothelial valvular dysfunction, recruitment of inflammatory cells, and thrombogenicity, as indicated by the pronounced protective effect of empagliflozin. Such beneficial effect is most likely attributable to the high effectiveness of empagliflozin to impede the sustained pro-oxidant activator signal and NF-κB activation. If VECs constitute a source of SGLT2 within the pathological valve, inflammatory cells, such as monocytes, could also likely express functional SGLT2 and promote redox signaling.[33] Overall, our data extend previous works demonstrating the potent antioxidant and inflammatory properties of SGLT2i in the vasculature[25] and highlight their potential relevance in preventing valvular dysfunction.

STUDY LIMITATIONS. The collection of human nonpathological valves as a control was unattainable. In this study, human AR valves were used as a control. However, the number of human AR valves collected was limited. Platelet-derived EVs were identified using GpIb antibody, which limits the identification of EVs from platelets that have undergone ADAM17-mediated GpIb shedding upon activation/EV release. In vivo interactions between EVs and native valve or prosthetic ones were not investigated. Finally, the impact of shear stress in the regulation of EV-VEC interactions was not assessed.

CONCLUSIONS

Calcified AS valve is a potent reservoir of EVs, acting as a prothrombogenic source per se and prompting VEC dysfunction through redox activation of the AT1R/NADPH oxidases/SGLT2 pathways. The observed protective effect of empagliflozin suggests SGLT2 inhibitors as a novel therapeutic option to curb valve dysfunction.

FUNDING SUPPORT AND AUTHOR DISCLOSURES

This work was supported by an unrestricted research grant by the Groupe pour l'Enseignement de la Recherche Cardio-vasculaire en Alsace, France. The authors have reported that they have no relationships relevant to the contents of this paper to disclose.

ADDRESS FOR CORRESPONDENCE: Prof Olivier Morel, Nouvel Hôpital Civil, University Hospital of Strasbourg, 1 Place de l'Hôpital, 67000 Strasbourg, France. E-mail: olivier.morel@chru-strasbourg.fr.

PERSPECTIVES

COMPETENCY IN MEDICAL KNOWLEDGE: In the time course of aortic stenosis, aortic valve constitutes per se a pool of prothrombotic factors, including EVs. Besides their prothrombotic activity, intravalvular EVs are involved in the different steps of aortic stenosis pathogenesis including valvular endothelium dysfunction, inflammation, and calcification.

TRANSLATIONAL OUTLOOK 1: The comprehension of prothrombotic mechanisms during aortic stenosis and after transcatheter aortic valve replacement is of paramount importance to develop therapeutic strategies to limit thrombotic risk and to curb valvular dysfunction.

TRANSLATIONAL OUTLOOK 2: The protective role of SGLT2 inhibition by empagliflozin demonstrated in this study suggests a potential novel therapeutic option required to be investigated in clinical studies to delay aortic stenosis evolution.

REFERENCES

1. Goody PR, Hosen MR, Christmann D, et al. Aortic valve stenosis. *Arterioscler Thromb Vasc Biol*. 2020;40(4):885–900.

2. Lindman BR, Clavel MA, Mathieu P, et al. Calcific aortic stenosis. *Nat Rev Dis Primer*. 2016;2:16006.

3. Trimaille A, Hmadeh S, Matsushita K, Marchandot B, Kauffenstein G, Morel O. Aortic stenosis and the hemostatic system. *Cardiovasc Res*. 2023;119(6):1310–1323.

4. Sellers SL, Turner CT, Sathananthan J, et al. Transcatheter aortic heart valves: histological analysis providing insight to leaflet thickening and structural valve degeneration. *JACC Cardiovasc Imaging*. 2019;12(1):135–145.

5. Hein M, Schoechlin S, Schulz U, et al. Long-term follow-up of hypoattenuated leaflet thickening after transcatheter aortic valve replacement. *JACC Cardiovasc Interv*. 2022;15(11):1113–1122.

6. Kwiecinski J, Tzolos E, Cartlidge TRG, et al. Native aortic valve disease progression and bioprosthetic valve degeneration in patients With transcatheter aortic valve implantation. *Circulation*. 2021;144:1396–1408.

7. Morel O, Toti F, Hugel B, et al. Procoagulant microparticles: disrupting the vascular homeostasis equation? *Arterioscler Thromb Vasc Biol*. 2006;26(12):2594–2604.

8. Abbas M, Jesel L, Auger C, et al. Endothelial microparticles from acute coronary syndrome patients induce premature coronary artery endothelial cell aging and thrombogenicity: role of the Ang II/AT1 receptor/NADPH oxidase-mediated activation of MAPKs and PI3-kinase pathways. *Circulation*. 2017;135(3):280–296.

9. Chen X, Andresen1 BT, Hill M, Zhang J, Booth F, Zhang C. Role of reactive oxygen species in tumor necrosis factor-alpha induced endothelial dysfunction. *Curr Hypertens Rev*. 2008;4(4):245–255.

10. Fu M, Yu J, Chen Z, et al. Epoxyeicosatrienoic acids improve glucose homeostasis by preventing NF-κB-mediated transcription of SGLT2 in renal tubular epithelial cells. *Mol Cell Endocrinol*. 2021;523:111149.

11. Dweck MR, Jones C, Joshi NV, et al. Assessment of valvular calcification and inflammation by positron emission tomography in patients with aortic stenosis. *Circulation*. 2012;125(1):76–86.

12. Stein PD, Sabbah HN, Pitha JV. Continuing disease process of calcific aortic stenosis. Role of microthrombi and turbulent flow. *Am J Cardiol*. 1977;39(2):159–163.

13. Andreasen C, Gislason GH, Køber L, et al. Incidence of ischemic stroke in individuals with and without aortic valve stenosis. *Stroke*. 2020;51(5):1364–1371.

14. Bogyi M, Schernthaner RE, Loewe C, et al. Subclinical leaflet thrombosis after transcatheter aortic valve replacement: a meta-analysis. *JACC Cardiovasc Interv*. 2021;14(24):2643–2656.

15. Trimaille A, Hmadeh S, Morel O. Letter by Trimaille et al regarding article, "native aortic valve disease progression and bioprosthetic valve degeneration in patients with transcatheter aortic valve implantation." *Circulation*. 2022;145(15):e807-e808.

16. Diehl P, Nagy F, Sossong V, et al. Increased levels of circulating microparticles in patients with severe aortic valve stenosis. *Thromb Haemost*. 2008;99(4):711–719.

17. Horn P, Stern D, Veulemans V, et al. Improved endothelial function and decreased levels of endothelium-derived microparticles after transcatheter aortic valve implantation. *EuroIntervention*. 2015;10(12):1456–1463.

18. Blaser MC, Buffolo F, Halu A, et al. Multiomics of tissue extracellular vesicles identifies unique modulators of atherosclerosis and calcific aortic valve stenosis. *Circulation*. 2023;148(8):661–678.

19. Yang X, Fullerton DA, Su X, Ao L, Cleveland JC, Meng X. Pro-osteogenic phenotype of human aortic valve interstitial cells is associated with higher levels of Toll-like receptors 2 and 4 and enhanced expression of bone morphogenetic protein 2. *J Am Coll Cardiol*. 2009;53(6):491–500.

20. Bouchareb R, Boulanger MC, Fournier D, Pibarot P, Messaddeq Y, Mathieu P. Mechanical strain induces the production of spheroid mineralized microparticles in the aortic valve through a RhoA/ROCK-dependent mechanism. *J Mol Cell Cardiol*. 2014;67:49–59.

21. Richards J, El-Hamamsy I, Chen S, et al. Side-specific endothelial-dependent regulation of aortic valve calcification: interplay of hemodynamics and nitric oxide signaling. *Am J Pathol*. 2013;182(5):1922–1931.

22. Jerez-Dolz D, Torramade-Moix S, Palomo M, et al. Internalization of microparticles by platelets is partially mediated by toll-like receptor 4 and enhances platelet thrombogenicity. *Atherosclerosis*. 2020;294:17–24.

23. Nakashima T, Umemoto S, Yoshimura K, et al. TLR4 is a critical regulator of angiotensin II-induced vascular remodeling: the roles of extracellular SOD and NADPH oxidase. *Hypertens Res*. 2015;38(10):649–655.

24. Venardos N, Deng XS, Yao Q, et al. Simvastatin reduces the TLR4-induced inflammatory response in human aortic valve interstitial cells. *J Surg Res*. 2018;230:101.

25. Park SH, Belcastro E, Hasan H, et al. Angiotensin II-induced upregulation of SGLT1 and 2 contributes to human microparticle-stimulated endothelial senescence and dysfunction: protective effect of gliflozins. *Cardiovasc Diabetol*. 2021;20:65.

26. Choi B, Lee S, Kim SM, et al. Dipeptidyl peptidase-4 induces aortic valve calcification by inhibiting insulin-like growth factor-1 signaling in valvular interstitial cells. *Circulation*. 2017;135(20):1935–1950.

27. Yu C, Zhang C, Kuang Z, Zheng Q. The role of NLRP3 inflammasome activities in bone diseases and vascular calcification. *Inflammation*. 2021;44(2):434–449.

28. Helske S, Lindstedt KA, Laine M, et al. Induction of local angiotensin II-producing systems in stenotic aortic valves. *J Am Coll Cardiol*. 2004;44(9):1859–1866.

29. O'Brien KD, Shavelle DM, Caulfield MT, et al. Association of angiotensin-converting enzyme with low-density lipoprotein in aortic valvular lesions and in human plasma. *Circulation*. 2002;106(17):2224–2230.

30. Peltonen T, Näpänkangas J, Ohtonen P, et al. (Pro)renin receptors and angiotensin converting enzyme 2/angiotensin-(1-7)/Mas receptor axis in human aortic valve stenosis. *Atherosclerosis*. 2011;216(1):35–43.

31. Bull S, Loudon M, Francis JM, et al. A prospective, double-blind, randomized controlled trial of the angiotensin-converting enzyme inhibitor Ramipril In Aortic Stenosis (RIAS trial). *Eur Heart J Cardiovasc Imaging*. 2015;16(8):834–841.

32. Mazur P, Kopytek M, Ząbczyk M, Undas A, Natorska J. Towards personalized therapy of aortic stenosis. *J Pers Med*. 2021;11(12):1292.

33. Semo D, Obergassel J, Dorenkamp M, et al. The sodium-glucose co-transporter 2 (SGLT2) inhibitor empagliflozin reverses hyperglycemia-induced monocyte and endothelial dysfunction primarily through glucose transport-independent but redox-dependent mechanisms. *J Clin Med*. 2023;12(4):1356.

KEY WORDS aortic stenosis, extracellular vesicles, inflammation, leaflet, microparticles, SGLT2i, SVD, TAVI, TAVR, thrombosis

APPENDIX For an expanded Methods section as well supplemental figures and tables, please see the online version of this paper.